Molecular and Channel-Forming Characteristics of Gramicidin K's: A Family of Naturally Occurring Acylated Gramicidins†

Linda P. Williams, Elizabeth J. Narcessian, and Olaf S. Andersen*

Department of Physiology and Biophysics, Cornell University Medical College, New York, New York 10021

George R. Waller

Department of Biochemistry, Oklahoma State University, Stillwater, Oklahoma 74074

M. Jeffrey Taylor, John P. Lazenby, James F. Hinton, and Roger E. Koeppe, II*

Department of Chemistry and Biochemistry, University of Arkansas, Fayetteville, Arkansas 72701

Received November 25, 1991; Revised Manuscript Received April 8, 1992

ABSTRACT: The gramicidin K family is a set of naturally occurring acylated linear peptides in which a fatty acid is esterified to the ethanolamine hydroxyl of either gramicidin A or C, and possibly also to gramicidin B (Koeppe, R. E., II, Paczkowski, J. A., & Whaley, W. L. (1985) *Biochemistry 24*, 2822–2826). These acylated gramicidins form membrane-spanning channels in planar lipid bilayers and therefore constitute a model system with which to study the structural and functional consequences of acylation on membrane proteins. This paper serves to characterize further the channels formed by acylated gramicidins A and C and to demonstrate that these channels are structurally equivalent to the channels formed by the standard gramicidins. We also present additional evidence for the ester linkage in the natural acylated gramicidins A and C and identify the fatty acyl chains.

The linear gramicidins, as exemplified by gramicidin A (gA),[1] are peptide antibiotics produced by *Bacillus brevis* with the following general structure (Sarges & Witkop, 1965): formyl-L-Xxx[1]-Gly[2]-L-Ala[3]-D-Leu[4]-L-Ala[5]-D-Val[6]-L-Val[7]-D-Val[8]-L-Trp[9]-D-Leu[10]-L-Yyy[11]-D-Leu[12]-L-Trp[13]-D-Leu[14]-L-Trp[15]-ethanolamine, where Xxx denotes Val or Ile and Yyy denotes Trp, Phe, and Tyr in gA, gB, and gC, respectively. The gramicidins form cation-selective channels in biological membranes, planar bilayers, and lipid vesicles [e.g., see Sawyer et al. (1990) for a comparison of gA, gB, and gC channels]. The gramicidin family has been used extensively as a set of prototypical channel-forming molecules to examine the mechanism of ion transport, lipid–protein interactions [e.g., Pullman et al. (1988)], and the mechanism of channel assembly (O'Connell et al., 1990).

Recently, gramicidin analogues containing a fatty acyl chain, most probably esterified to the ethanolamine hydroxyl group, were described (Koeppe et al., 1985). In this article we more fully characterize the structural and channel-forming properties of these acylated gramicidins. Preliminary reports of some of this work have appeared (Koeppe et al., 1988; Williams et al., 1988).

EXPERIMENTAL PROCEDURES

Materials. Linear gramicidin was purchased from U. S. Biochemical Corp. (Cleveland, OH). Myristic acid ethyl ester was from Sigma Chemical Co. (St. Louis, MO). Other materials were as previously described (Koeppe et al., 1990).

Methods. Acylated gramicidins were isolated from commercial preparations of linear gramicidins from *Bacillus brevis* by the methods of Koeppe et al. (1985). When the period for the collection of fractions was extended, acylated forms of gB, as well as gA and gC, were obtained (Figure 1).

Individual fractions from chromatograms similar to Figure 1 either were repurified on high-resolution octyl-silica columns for single-channel analysis [see Koeppe et al. (1985, 1990)] or were vacuum dried, resuspended in the appropriate solvent, and used for NMR or base hydrolysis studies.

Single-channel current measurements were done in planar bilayer membranes using the bilayer punch (Andersen, 1983a).

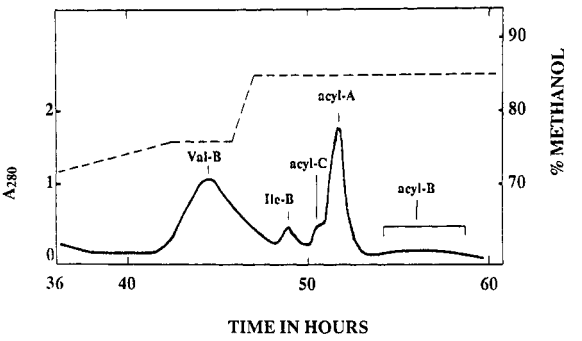

FIGURE 1: Late fractions in the resolution of a 300-mg sample of commercial linear gramicidins on a 0.45 × 100 cm column followed by a 0.78 × 240 cm column of Chromosorb LC-5. Fractions were eluted at 27 mL/h for 26 h with 68% methanol and for 10 h with 72% methanol prior to the gradient shown. Peaks containing [Val[1]]- and [Ile[1]]gramicidin B, and acylgramicidins C, A, and B are indicated. For the elution profile of the earlier fractions (nonacylated gramicidins C and A), see Figure 1 of Koeppe et al. (1985).

† This work was supported in part by Grants GM-21342 (O.S.A.) and GM-34968 (R.E.K.) from the NIH. The NMR spectrometer was purchased through grants from the U.S. Department of Education (J.F.H.) and the Arkansas Science and Technology Authority (J.F.H.).

[1] Abbreviations: gA, gramicidin A; gB, gramicidin B; gC, gramicidin C; DMSO, dimethyl sulfoxide; DPhPC, diphytanoylphosphatidylcholine; F_3Val, 4,4,4-trifluorovaline.

0006-2960/92/0431-7311$03.00/0

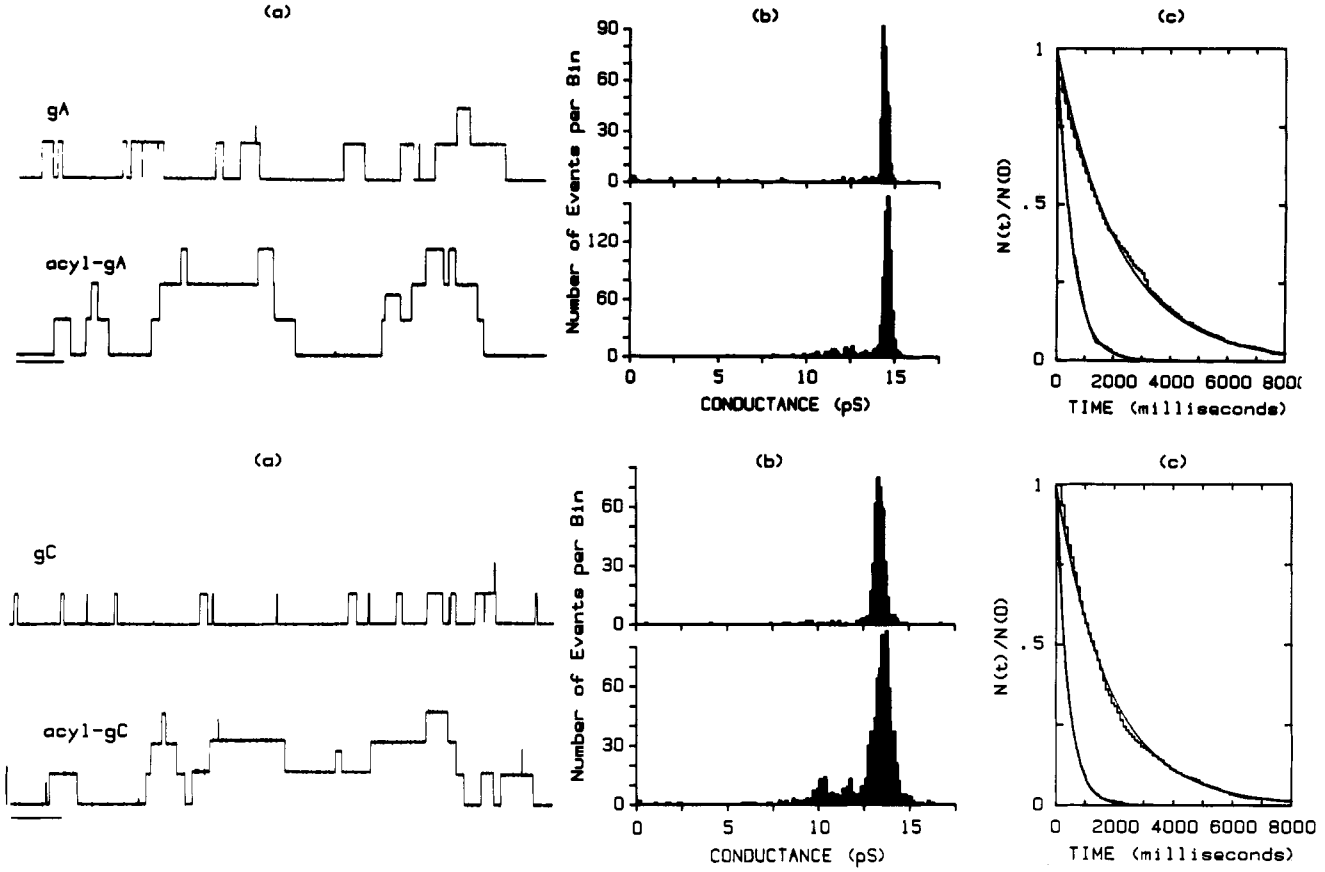

FIGURE 2: Current tracings, conductance histograms, and duration histograms for channels formed by gA and acyl-gA (top) and by gC and acyl-gC (bottom), at 200 mV. (a) Single-channel current traces, from top to bottom: gA, acyl-gA, gC, and acyl-gC. Calibration bars: 15 pS (vertically), 2 s (horizontally). (b) Conductance histograms. For gA, there are 371 transitions in the histogram, of which 331 (89%) are in the main peak at 14.4 ± 1.5 pS. For acyl-gA, there are 781 transitions in the histogram, of which 645 (83%) are in the main peak at 14.5 ± 0.2 pS (mean ± standard deviation). For gC, there are 415 transitions in the histogram, of which 383 (92%) are in the main peak at 13.3 ± 0.3 pS. For acyl-gC, there are 910 transition in the histogram, of which 746 (82%) are in the main peak at 13.5 ± 0.5 pS. (c) Duration histograms. Top, gA and acyl-gA channels: for gA channels, τ = 540 ms (N = 542); for acyl-gA channels, τ = 2200 ms (N = 966). Bottom, gC and acyl-gC channels: for gC channels, τ = 420 ms (N = 580); for acyl-gC channels, τ = 1800 ms (N = 1097). 1.0 M NaCl, 200 mV.

The bilayers were formed from diphytanoylphosphatidylcholine (DPhPC) suspended in *n*-decane (2–3% w/v) at 25 ± 1 °C. The electrolyte solution was unbuffered 1.0 M NaCl, which was made up the day of the experiment. The experimental procedures and analysis were as described previously (Andersen, 1983a; Sawyer et al., 1989; Durkin et al., 1990).

Base Hydrolysis. The acylated gramicidins were subjected to mild base hydrolysis by treating 0.1-mg samples with 0.06 M NaOH in 85% methanol (0.5 mL) at room temperature for 12 h. The resulting peptides were isolated (from some samples) by chromatography on a 4.6 × 250 mm Zorbax C_8 HPLC column (DuPont) at 1800 psi using 83% methanol at room temperature. Fatty acids were extracted (from the remaining samples) by acidifying the NaOH-treated samples to pH 2 with HCl, removing the solvent, and transferring the methylene chloride-soluble portion of the residue to a glass vial. After removal of the methylene chloride, the fatty acids were converted to methyl esters using diazomethane (Cast et al., 1990). Low-resolution mass spectra of the diazomethane-treated samples were obtained using an LKB-2091 (LKB Produckter, Bromma, Sweden) capillary gas chromatograph–mass spectrometer–data analysis system (CGC–MS–DAS) (McGown & Waller, 1986). The column was 30 m × 0.25 mm DB-5 (J&W Scientific, Folsom, CA), operated at an injection temperature of 100 °C, followed by a programmed temperature rise (after 4 min) of 10 °C/min until 280 °C was reached, and then 15 min at 280 °C. Mass spectra of the eluting fractions were recorded every 1.18 s. The spectra were compared with known spectra as listed in the Eight Peak Index of Mass Spectra (1983).

NMR Spectroscopy. For ^{13}C-nuclear magnetic resonance (^{13}C-NMR) spectroscopy, 10 mg of acyl-gA was dissolved in 0.7 mL of 99.96% dimethyl-d_6 sulfoxide (MSD Isotopes, St. Louis, MO). Spectra were recorded on a 500-MHz Varian VXR 500S spectrometer.

RESULTS

Fundamental Channel Properties. The acylated gramicidins form channels that, except for two features, are similar to those formed by the standard gramicidins (Figure 2). While the general shape of the single-channel current transitions and the majority of the current transition amplitudes are similar for acyl-gA and acyl-gC, as compared to gA and gC (Figure 2a and b), the current transition amplitude distributions display a larger conductance heterogeneity for the channels formed by the acylated gramicidins (Figure 2b). The most dramatic difference, however, between channels formed by the standard and the acylated gramicidins is in the channel durations. For all the channel types, the survivor plots of the durations (Cox & Lewis, 1965) are described by single-exponential decays [$N(t) = N(0) \exp\{-t/\tau\}$], but the average durations (τ) are *4-fold longer* for channels formed by the acylated gramicidins (Figure 2c).

The increased conductance heterogeneity is observed at all potentials (cf. Figure 2b and Figure 3). When the conductance

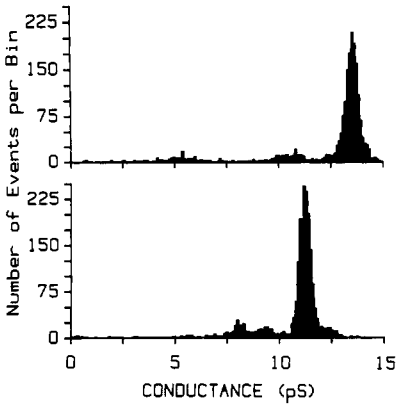

FIGURE 3: Current transition histograms for channels formed by acyl-gA (top) and acyl-gC (bottom); cf. Sawyer et al. (1989). For acyl-gA channels, there are 1967 channels in the histogram, of which 1515 (77%) are in the main peak at 13.5 ± 4 pS (mean ± standard deviation). For acyl-gC channels, there are 2179 channels in the histogram, of which 1662 (76%) are in the main peak at 11.2 ± 0.3 pS. 100 mV.

heterogeneity was quantified, the minichannel frequency (f_m)[2] varied more than 2-fold (from ~15% to ~35%). The relative variation is comparable to that observed for channels formed by the standard gramicidins (Sawyer et al., 1989), but f_m is ~3-fold larger than we usually observe for the latter channels. The increase in f_m could be a result of the acylation, but that is probably not the case because chemically acylated gA (Vogt et al., 1992) forms channels that have f_m that is similar to that of gA channels. In particular, we cannot exclude the possibility that some of the conductance dispersity could result from an admixture of gramicidins having different amino acid sequences (as evidenced by the fairly broad peaks in the chromatogram of Figure 1, where [Ile[1]]gB elutes close to acyl-gC). In any case, it is not clear whether the acylation directly causes the appearance of minichannels or merely facilitates their formation in the presence of other variable factors in the membrane environment (Sawyer et al., 1989).

The increases in τ (i.e., in channel stability) are consistent with the notion that the acylated gramicidins are more hydrophobic than the standard compounds. One would likewise expect that the acylated gramicidins should be better channel formers than the standard gramicidins. But that is not the case: Relative to gA and gC, it was necessary to add ~10-fold more of acyl-gA or acyl-gC in order to have similar channel activities (channel appearances per second); see also Vogt et al. (1992).

Structural Equivalence of Gramicidin Channels and Acyl Gramicidin Channels. The general similarity between the channels formed by the acylated gramicidins and those formed by the standard gramicidins suggests in itself that the former channels are quite similar to the latter, i.e., being (formyl-NH-terminal)-to-(formyl-NH-terminal) $\beta^{6.3}$-helical dimers, as originally proposed by Urry (1971). But the presence of the acyl chain could alter the normal folding and, for example, change the helix sense from right-handed (Arseniev et al., 1985, 1986; Nicholson et al., 1989; Koeppe et al., 1992) to left-handed. The ethanolamine moiety has in fact been implicated as being important for normal function (Etchebest & Pullman, 1984, 1986; Etchebest et al., 1984). Less likely, the acyl chain could alter monomer–monomer association.

[2] The minichannel frequency f_m is defined as $100(1 - n_{standard}/n_{tot})$, where $n_{standard}$ denotes the number of events in the major peak in the amplitude histogram and n_{tot} the total number of events in the histogram [cf. Busath et al. (1987)].

In order to examine these questions further, we tested the ability of the acylgramicidins to form hybrid channels with appropriate reference compounds. Quantitative analysis of hybrid and symmetrical channel appearances and durations allows calculation of the difference in free energy of formation ($\Delta\Delta G^{\ddagger}$) and of stability ($\Delta\Delta G°$) for the heterodimeric channels relative to the homodimeric channels in the same membrane (Durkin et al., 1990):

$$\Delta\Delta G^{\ddagger} = RT \ln \{f_h/[2(f_a f_b)^{0.5}]\} \quad (1)$$

and

$$\Delta\Delta G° = RT \ln \{f_h \tau_h/[2(f_a \tau_a f_b \tau_b)^{0.5}]\} \quad (2)$$

where the f's denote the channel appearance rates, the subscripts denote the heterodimers (h) and homodimers (a and b), and the $\Delta\Delta G$'s are measured relative to the average of the ΔG's for the two symmetrical channels. The essential assumptions of this analysis are that gramicidin monomers and dimers in the membrane are in equilibrium and that both monomers are distributed symmetrically between the two monolayers (Durkin et al., 1990).

The similar single-channel conductances for channels formed by the standard gA and acyl-gA, however, make hybrid channel analysis difficult because one can only distinguish the different channel types by their different average durations, which is an intrinsically less accurate procedure. In order to circumvent this problem we used an analogue, [F_3Val[1]]gA, that forms channels that have a smaller conductance that gA channels (Russell et al., 1986) but the same structure as gA channels (Durkin et al., 1990). Because hybrid channel formation is a transitive property (Durkin et al., 1990), it will suffice to show that acyl-gA channels are structurally equivalent to [F_3Val[1]]gA channels.

Figure 4 illustrates single-channel current tracings and amplitude histograms obtained with acyl-gA, with [F_3Val[1]]gA, and with their mixture. With the mixture, a new channel type of intermediate conductance is evident in the current traces (Figure 4a). These new channel events are only observed when both gramicidins are present; they are therefore heterodimers (hybrid channels). There is likewise a new peak in the amplitude histogram (Figure 4a), between the two pure channel peaks, that corresponds to the hybrid channels formed by the two chemically dissimilar peptides.

The frequency of hybrid channel formation relative to that of the symmetrical channel types [$f_h/[2(f_a f_b)^{0.5}]$, Durkin et al. (1990)] is 1.4 ± 0.2 (mean ± standard error of mean, n = 8), indicating that the hybrid channels form readily ($\Delta\Delta G^{\ddagger}$ = –0.8 kJ/mol or within $RT/2$ of zero). This indicates that no refolding is necessary to order to form acyl-gA/[F_3Val[1]]gA heterodimers relative to acyl-gA homodimers (Durkin et al., 1990). We therefore conclude that acyl-gA forms channels that have the same structure as channels formed by [F_3Val[1]]gA and, by extension, channels formed by gA itself. $\Delta\Delta G°$ = –0.9 kJ/mol (Figure 4c and eq 2), which shows that the acylation does not introduce a strain at the join between the two monomers. This latter result shows also that the acylation cannot be at the formyl-NH terminus.

Ester Linkage. The acylgramicidins have the same amino acid compositions as the respective nonacylated gramicidins (Koeppe et al., 1985). The fatty acid cannot be attached at the formyl-NH_2 terminus (see above); it is therefore most likely attached at the ethanolamine OH group. Indeed, the fatty acyl linkage is an ester bond, as evidenced by the ^{13}C-chemical NMR shift of the extra carbonyl carbon in the acyl-

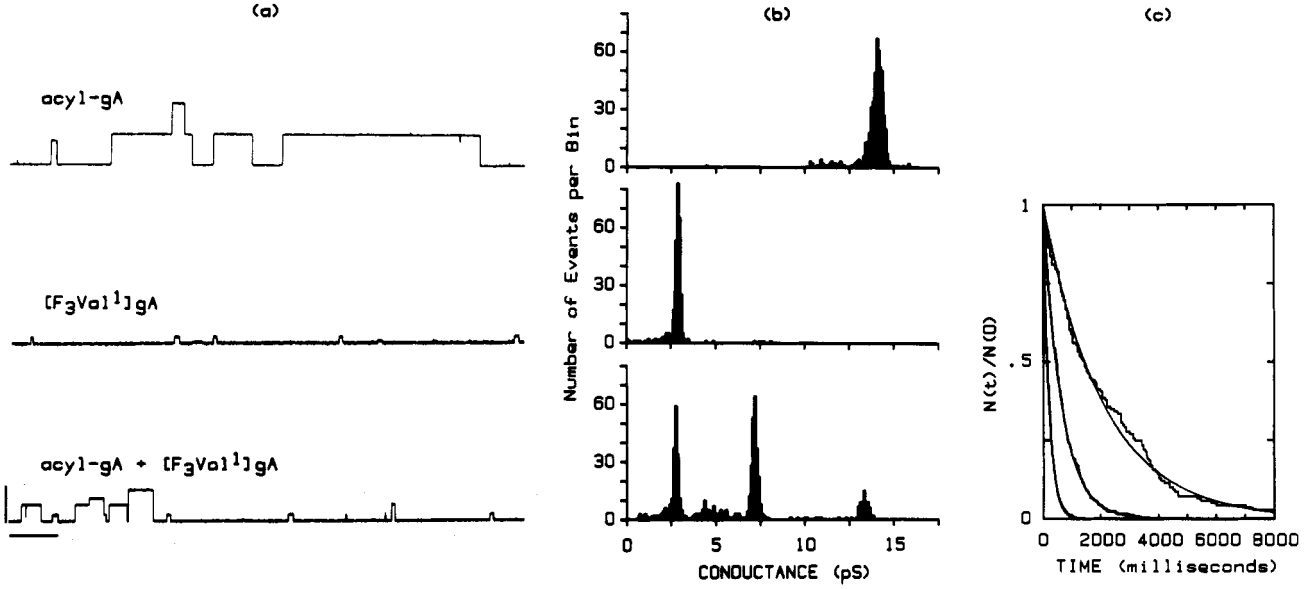

FIGURE 4: Hybrid channel experiment. Heterodimers form between acyl-gA and [F_3Val^1]gA; 100 mV. (a) Single-channel current traces obtained with only acyl-gA (top), with only [F_3Val^1]gA (middle), and with their mixture (bottom). Both symmetrical channel types appear in the bottom trace as well as a new channel type, the hybrid channels (or heterodimers), which only appear when both gramicidins are present. The calibration bars denote 10 pS (vertically) and 2 s (horizontally). (b) Conductance histograms obtained with only acyl-gA (top), [F_3Val^1]gA (middle), and with their mixture (bottom). The top histogram contains 500 transitions, of which 453 (or 91%) are in the main peak at 14.0 ± 0.3 pS (mean ± standard deviation). The middle histogram contains 289 transitions, of which 250 (or 87%) are in the main peak at 2.8 ± 0.1 pS. The bottom histogram contains 591 transitions: 173 (29%) are in the [F_3Val^1]gA channel peak at 2.7 ± 0.2 pS; 234 (40%) are in the hybrid channel peak at 7.1 ± 0.2 pS; and 63 (11%) are in the acyl-gA channel peak at 13.4 ± 0.2 pS. (c) Survivor histograms for the three channel types observed in these experiments: for acyl-gA channels, τ = 2100 ms (N = 135); for the hybrid channels, τ = 630 ms (N = 227); for [F_3Val^1]gA channels, τ = 200 ms (N = 340). $\tau_h/(\tau_{acyl\text{-}gA}\tau_{[F3Val^1]gA})$ = 0.97.

gramicidin. Figure 5 shows the carbonyl region of the ^{13}C-NMR spectrum of acyl-gA.

A new carbonyl resonance, not present in the spectrum of gA, is evident at 172.81 ppm. The assignment of this peak to an ester carbonyl is consistent with the resonance at 172.88 ppm in the ^{13}C-NMR spectrum of myristic acid ethyl ester (Figure 6). The ester carbonyl resonance frequency is downfield from all of the amide carbonyl frequencies.

The resonance frequencies for the formyl and glycine carbonyl carbons of gA in DMSO are not affected by the presence of an acyl group (Table I). By contrast, the Trp^{15} carbonyl frequency is shifted upfield, from 171.73 to 171.44 ppm, in the presence of the acyl group. The result suggests that the formyl-NH terminal of the gramicidins is largely unaffected by acylation, in general agreement with the conclusion from the hybrid channel experiments.

Release of Acyl Chains. When acylgramicidins are treated with mild base (see Methods), the products are a mixture of at least four fatty acids together with peptides that resemble the natural [Val^1]- and [Ile^1]gA, -gB, and -gC from *B. brevis*. Figure 7 shows a HPLC chromatogram for the base-hydrolyzed acylgramicidin mixture. Peaks due to [Val^1]- and [Ile^1]gA and -gC, as well as [Val^1]gB are apparent in the tracing.

Channels Formed by the Base-Hydrolyzed Gramicidins. In order to further verify the identity of the base-hydrolysis products, we examined whether they could form channels and then characterized their single-channel properties. The current traces, amplitude histograms, and duration distributions (Figure 8) are similar to those for channels formed by the standard gramicidins (Figure 2). The differences in channel durations between standard gramicidin channels and acyl-chain-removed channels (540 versus 770 ms for the gA's and 420 versus 280 ms for the gC's) are, in particular, no larger than can be accounted for by day-to-day variations [cf. Table 3 in Durkin et al. (1990)]. We conclude that the originally observed duration differences (Figure 2) were due to the acyl chains and not to the peptide portions of the channels.

Fatty Acid Components. The non-peptide products of the base hydrolysis were analyzed by CGC–MS–DAS. (To improve resolution and separation, the acids were converted to the methyl esters using diazomethane.) Four major products are evident in the gas chromatogram of Figure 9. There are also minor peaks, but they do not obviously correspond to fatty acids or their derivatives and have not been identified.

The major peaks were identified by their molecular ions, and by comparison with the Eight Peak Index of Mass Spectra (1983) as the methyl esters of pentadecanoic acid (m/z = 256), 12-methyltetradecanoic acid (m/z = 256), hexadecanoic acid (m/z = 270), and octadecanoic acid (m/z = 298). For all four compounds, the two most intense fragments were the ion at m/z = 74 due to the McLafferty rearrangement (McLafferty, 1959; Williams et al., 1964) and an ion at m/z = 87, both indicative of methyl esters. The branching of 12-methyltetradecanoic acid is indicated by the relatively high intensities of the fragment peaks at m/z = 57 and 55 (Figure 10), due to the $CH_3CH_2CH(CH_3)^+$ ion, and the same with loss of H_2.

The aliphatic region of the ^{13}C-NMR spectrum of acyl-gA is likewise indicative of major fatty acid components (Figure 11). Interspersed among the aliphatic side chain resonances are a number of new peaks in the acyl-gA spectrum that are not seen in the spectrum of nonacylated gA (Table II). Of special significance are the terminal methyl resonance at 11.1 ppm and the branched methyl resonance near 19.0 ppm. The latter is sandwiched among the four distinct Val-γ_1 peaks at 18.9 and 19.2–19.35 ppm that appear in the spectra of both gA and acyl-gA.

Many new methylene resonances are also present in the ^{13}C-NMR spectrum (Figure 11). Indeed there are too many discrete resonances to be accounted for by a single type of

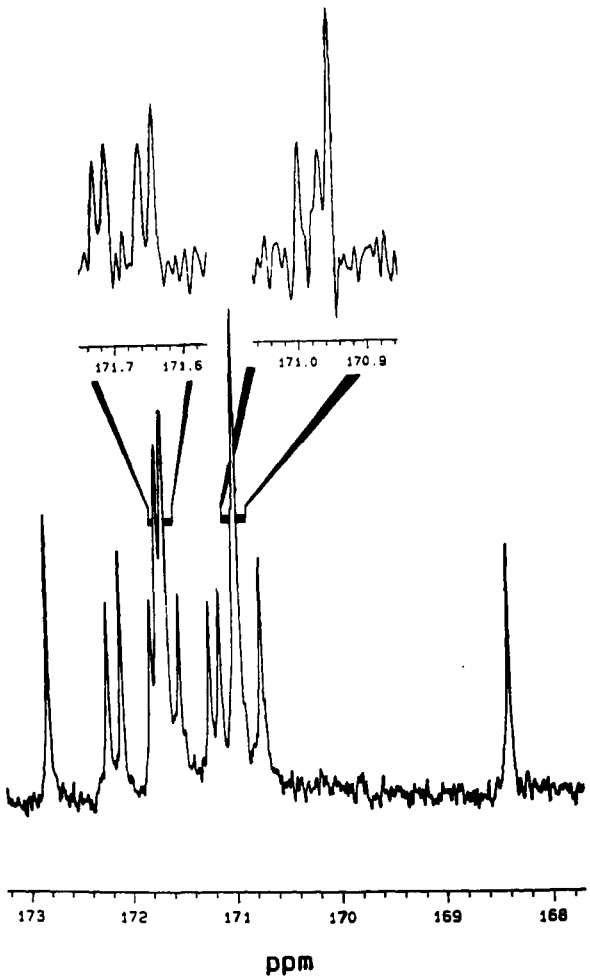

FIGURE 5: Carbonyl carbon region of ^{13}C-NMR spectrum of 7.5 mM acyl-gA dissolved in DMSO-d_6. The formyl carbon resonance at 161.13 ppm is not shown. Selected peak assignments are given in Table I. The ester carbonyl resonance is at 172.81 ppm. The insets are expansions to show individual resonances.

Table I: Chemical Shift Assignments for Selected Carbonyl Carbons of Acyl-gA in DMSO-d_6[a]

resonance, ppm		
acyl-gA	gA	assignment
161.13	161.18	formyl
168.40	168.45	Gly^2
171.73	171.44	Trp^{15}
172.81		fatty acyl ester

[a] Data for gA are from Hawkes et al. (1987). Acylation shifts the Trp^{15} carbonyl resonance and introduces a new one at 172.81 ppm. All others are unchanged.

acyl chain, again reflecting the heterogeneity of the population. [This variation in acyl chain structure does not, however, result in any significant dispersion in the single-channel properties; see also Vogt et al. (1992).] For comparison, the methylene resonances of myristic acid ethyl ester may be seen between 20 and 35 ppm in Figure 6. The general resonance pattern for acyl-gA is similar, but more complicated, even when the side-chain resonances of gA (Hawkes et al., 1987) are taken into account. The NMR results are thus consistent with multiple fatty acid components, as was previously indicated by GC–MS (see above; Figure 9).

DISCUSSION

We have previously reported the existence of a new class of gramicidins, the acylated gramicidins (Koeppe et al., 1985).

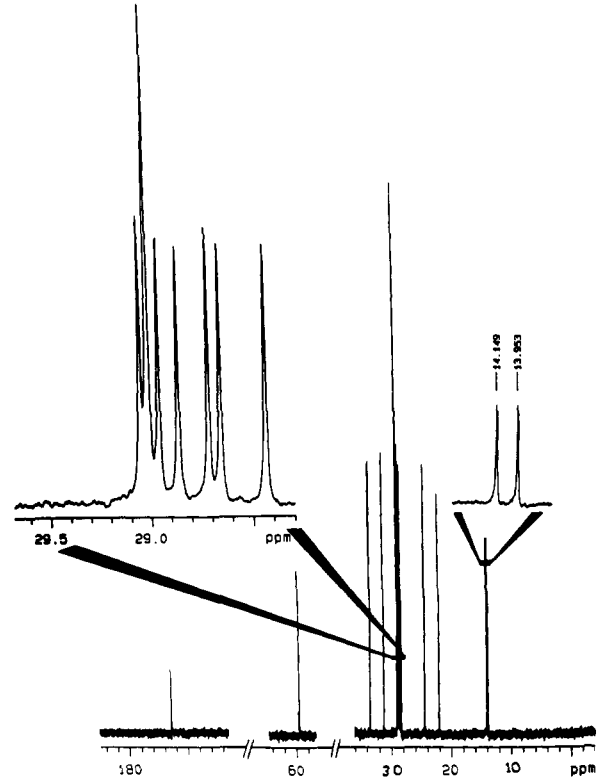

FIGURE 6: ^{13}C-NMR spectrum of 45 mM myristic acid ethyl ester dissolved in DMSO-d_6. The ester carbonyl resonance appears at 172.88 ppm. Aliphatic carbon resonances are evident in the region between 20 and 35 ppm.

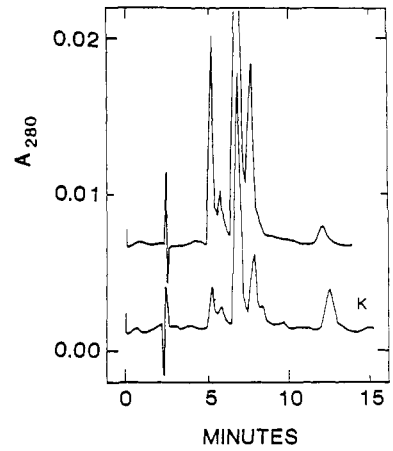

FIGURE 7: Comparison of the HPLC chromatogram for a base-hydrolyzed mixture of previously purified acylated gramicidin species (lower trace) with the chromatogram of a commercial mixture of [Val^1]- and [Ile^1]gA, -gB, and -gC (upper trace). Elution from a 4.6 × 250 mm column of Zorbax-C8 using 81% methanol, 19% water, 25 °C. Under these conditions the unhydrolyzed acyl-gramicidin components remain bound to the column indefinitely. Following the injection at time zero, the peaks on the upper trace represent, from left to right, solvent spike, [Val^1]gC, [Ile^1]gC, [Val^1]gA, [Ile^1]gA, and [Val^1]gB. The lower trace, due to the base-hydrolyzed mixture of acyl-gramicidins, is similar.

In this article, we have used a combination of functional and structural methods to further identify these compounds and to show that they are standard gramicidins that have a fatty acid esterified to the ethanolamine hydroxyl group.

We first discuss the general features of these acylated gramicidins and the channels they form, as compared with channels formed by the standard gramicidins. We then address the issue of the identity of the fatty acids. Finally, we speculate on the possible biological relevance of the acylation.

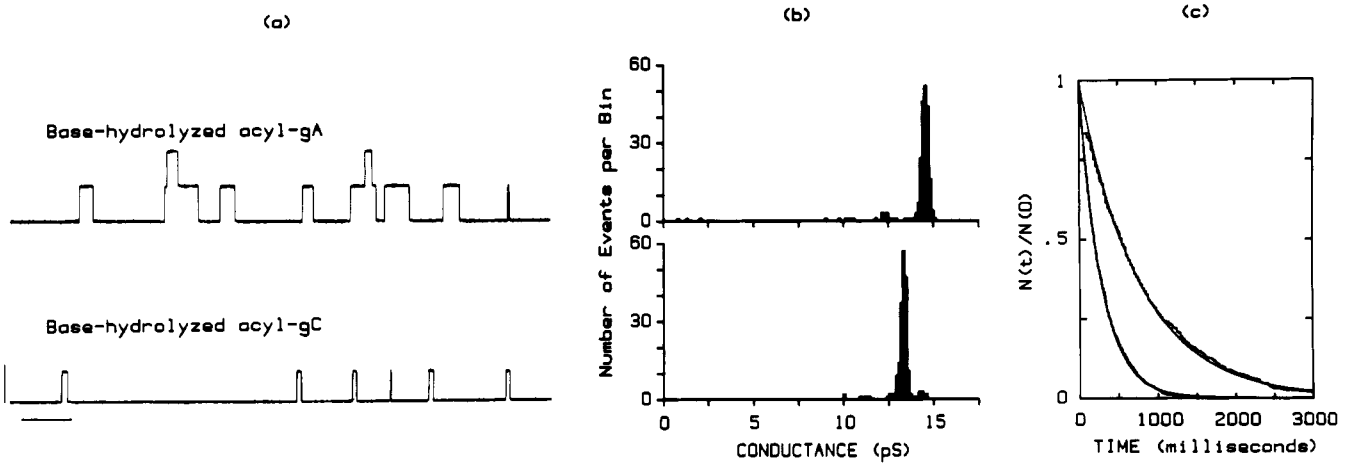

FIGURE 8: Single-channel analysis of the products from base hydrolysis of the acylated gramicidins. 200 mV. (a) Current traces for channels formed by HPLC-purified base-hydrolysis product of acyl-gA (top) and acyl-gC (bottom); cf. Figure 2. Calibration bars: 15 pS (vertical), 2 s (horizontal). (b) Conductance histograms. For the channels formed by base-hydrolyzed acyl-gA (top) there are 216 transitions in the histogram, of which 197 (91%) are in the main peak at 14.5 ± 0.2 pS (mean ± standard deviation). For the channels formed by base-hydrolyzed acyl-gC (bottom) there are 200 transitions in the histogram, of which 179 (90%) are in the main peak at 13.3 ± 0.15 pS. (c) Survivor plots for the two channel types. For the channels formed by the base-hydrolyzed acyl-gA, τ = 770 ms (N = 597); for the channels formed by the base-hydrolyzed acyl-gC, τ = 280 ms (N = 786).

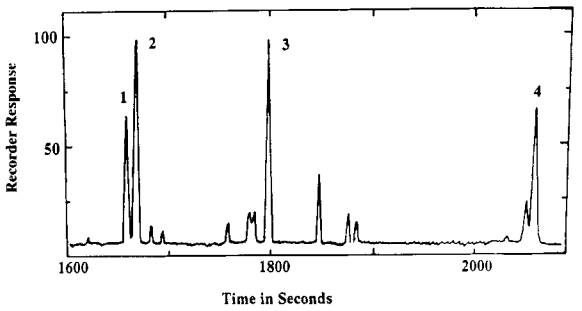

FIGURE 9: Partially reconstructed total ion current chromatogram of fatty acid methyl esters following base hydrolysis of acylated gramicidins, extraction, methylation, and analysis using the LKB-2091 CGC–MS–DAS. The four major peaks have been identified as representing the methyl esters of (1) pentadecanoic acid (m/z = 256), (2) 12-methyltetradecanoic acid (m/z = 256), (3) hexadecanoic acid (m/z = 270), and (4) octadecanoic acid (m/z = 298).

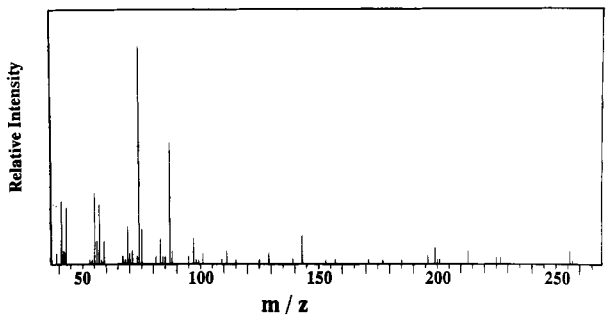

FIGURE 10: Mass spectrum that identifies peak 2 of Figure 9 as 12-methyltetradecanoic acid methyl ester (m/z = 256). The branching is indicated by the relatively high intensities of the peaks at m/z = 55 and 57.

Acylated Gramicidins. The chemical modification of the linear gramicidins that leads to the gramicidin K's is the esterification of a fatty acid to the ethanolamine hydroxyl. This was shown by several lines of evidence. First, the presence of a new carbonyl resonance in the ^{13}C-NMR spectrum is noted (Figure 5), with a chemical shift that is indicative of an ester linkage. Because there is only a single hydroxyl in gA, the ethanolamine OH, the location of the ester bond is specified. Second, the change in the ^{13}C-chemical shift for only the Trp^{15} carbonyl carbon, and no others (Table I), suggests that the acylation site is near the C terminal. Third, the presence of many new methylene resonances in the ^{13}C-NMR spectrum (Figure 11) suggests that the covalent modifiers are fatty acids. Fourth, milk alkaline hydrolysis converts the modified gramicidins back to the standard gramicidins, as evidenced by HPLC (Figure 7) and single-channel behavior (Figure 8), and releases a complex set of fatty acids (Figure 9 and 10).

Implications for Gramicidin Channels. The channels formed by the acylated gramicidins are structurally equivalent to standard gramicidin channels. This was shown qualitatively by their ability to form hybrid channels with [F$_3$Val^1]gA, and quantitatively by the finding that $\Delta\Delta G^{\pm}$ for hybrid channel formation was negative, but within $RT/2$ of zero (Figure 4). Consequently, there is no energetic barrier (peptide refolding) involved in the formation of the asymmetrical acyl-gA/[F$_3$Val^1]gA (heterodimeric) channels as compared to the formation of the symmetrical (homodimeric) acyl-gA channels (Durkin et al., 1990). Consequently, acylation at the ethanolamine hydroxyl group does not alter channel folding. Nor does the acylation alter ion permeation, as evidenced by the similar conductances of channels formed by the standard and acylated gramicidins (Figure 2).[3]

This finding is somewhat surprising, as conformational energy minimization has implicated the ethanolamine group as being important for channel folding as well as ion permeation (Etchebest & Pullman, 1984; Etchebest et al., 1984). From that point of view, these experiments expand on those reported by Trudelle et al. (1987), that removing the ethanolamine group and replacing it by an methylamine has little effect on channel function. This seeming lack of a functional effect of removing the OH group at the channel entrance is, however, consistent with the notion that the rate constant for ion entry into gramicidin channels is close to its diffusion-controlled limit (Andersen, 1983b). For gA channels, for example, the intrinsic rate constant for Na^+ association with the channel is ~6-fold larger than the diffusion-controlled rate constant

[3] Similar results have been obtained at other NaCl concentrations (0.1 M ≤ [NaCl] ≤ 5.0 M) and with Cs^+ as the permeant ion (0.1 M ≤ [CsCl] ≤ 5.0 M; E. J. Narcessian, L. P. Williams, O. S. Andersen, and R. E. Koeppe II, manuscript in preparation). See also Benayad et al. (1991).

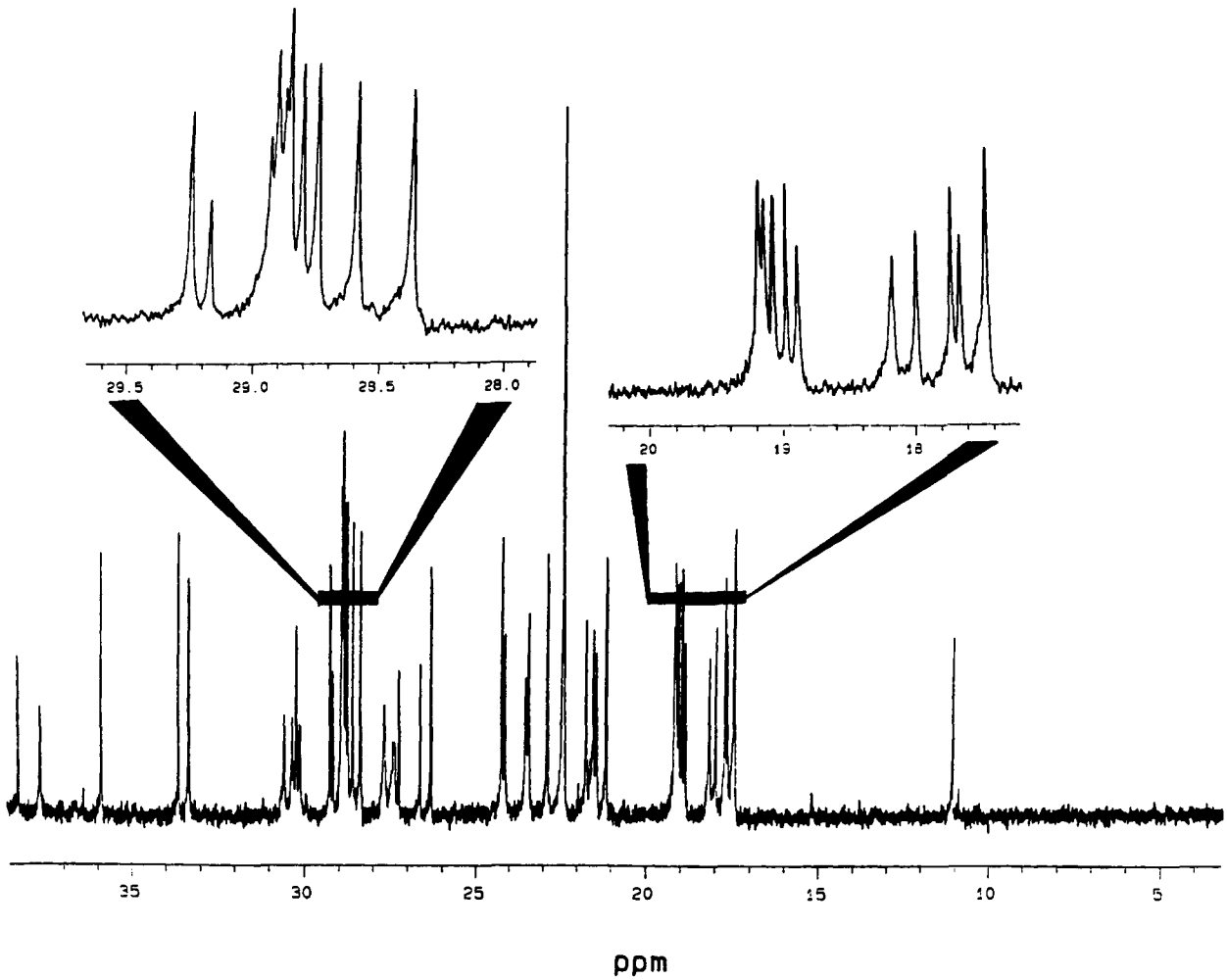

FIGURE 11: Aliphatic carbon region of ^{13}C-NMR spectrum of acyl-gA dissolved in DMSO-d_6. The cluster of five peaks between 18.8 and 19.4 ppm represents four Val-γ_1 methyl groups and a branched fatty acid methyl group (18.99 ppm). Numerous other aliphatic carbon peaks that are not present in the gA spectrum are at 24.16, 26.3–27.3, 28.4–29.3, and 33.3–38.4 ppm in the acyl-gA spectrum (see also Table II).

Table II: Chemical Shift Assignments for Selected Side-Chain and Fatty Acid Carbons of Acylgramicidin A in DMSO-d_6[a]

resonance, ppm			resonance, ppm		
acyl-gA	gA	assignment	acyl-gA	gA	assignment
11.10		terminal methyl	27.27		fatty acid
17.47	17.60	Cγ_2 Val	27.47	27.65	Cβ Trp
17.67	17.83	Cγ_2 Val	27.70	27.85	Cβ Trp
17.73	17.89	Cγ_2 Val	28.38		fatty acid
18.00	18.16	Cβ Ala	28.60		fatty acid
18.18	18.35	Cβ Ala	28.76		fatty acid
18.90	19.06	Cγ_1 Val	28.82		fatty acid
18.99		branched methyl	28.87		fatty acid
19.08	19.22	Cγ_1 Val	28.89		fatty acid
19.15	19.29	Cγ_1 Val	28.92		fatty acid
19.19	19.34	Cγ_1 Val	28.94		fatty acid
21.16	21.34	Cδ_1 Leu	29.18		fatty acid
21.45	21.58	Cδ_1 Leu	29.26		fatty acid
21.54	21.67	Cδ_1 Leu	30.12	30.30	Cβ Val
21.75	21.88	Cδ_1 Leu	30.23	30.37	Cβ Val
22.41	22.57	Cδ_2 Leu	30.35	30.49	Cβ Val
22.89	23.03	Cδ_2 Leu	30.57	30.74	Cβ Val
23.45	23.62	Cγ Leu	33.34		fatty acid
23.54	23.62	Cγ Leu	33.63		fatty acid
24.16		fatty acid	35.90		fatty acid
24.24	24.31	Cγ Leu	37.73		fatty acid
26.34		fatty acid	38.37		fatty acid
26.66		fatty acid			

[a] Data for gA are from Hawkes et al. (1987).

for Na^+ to encounter the entrance (Becker et al., 1992), which means that changes in the intrinsic association rate constant may have little if any effect on the single-channel conductance.

Even more suprising is the finding that the channel-forming potency is reduced while the average single-channel duration is increased by the acylation [see also Vogt et al. (1992)]. The latter result is what one would expect by introducing the nonpolar fatty acid into the channel structure—in which case the increased channel duration would be the result of an increased channel hydrophobicity. But the linear gramicidins are already among the most hydrophobic peptides/proteins known (Segrest & Feldmann, 1974), and it is not clear that the introduction of a fatty acid should have a significant effect on channel stability. A more interesting possibility is, therefore, that the introduction of the fatty acid alters the energetics of channel–membrane interactions.

The overall length of a gramicidin channel is ~2.6 nm (the length of the hydrophobic exterior surface is ~2.2 nm), which should be compared to an equilibrium thickness of ~4.5 nm for a DPhPC/*n*-decane bilayer in 1.0 M NaCl (Benz & Janko, 1976). Channel formation is thus associated with a membrane deformation (a local thinning), and the energetic cost of this membrane deformation will be reflected in the energetics and kinetics of channel formation. This problem has been analyzed using liquid-crystal theory (Huang, 1986; Helfrich & Jakobsson, 1990). One contribution to the deformation energy is bending (or splay), energy, which arises because the local bending of each monolayer in the vicinity of the channel introduces a differential expansion/compression along a normal to the surface. Qualitatively, this can be thought of

as a surface area/volume mismatch. We have previously shown that a variety of (micelle-forming) surface-active agents [e.g. lysophosphatidylcholine and Triton X-100 (Sawyer et al., 1989) and platelet-activating factor (Sawyer & Anderson, 1989)] increase the average channel duration ~5-fold when present at a detergent/lipid molar ratio of ~1/10. But each gramicidin channel is surrounded by 8–10 phospholipid molecules—the "extra" acyl chain would thus be present at an effective molar ratio of ~1/10, which for fairly short chains would serve to decrease the splay contribution to the energetic cost of channel formation.

These arguments do not, however, explain why acylation should decrease the overall channel formation rate [see also Vogt et al. (1992)]. We note, nevertheless, that this result can be rationalized within the framework at a scheme in which there are three membrane-associated forms of the gramicidin; cf. Cifu et al. (1992): conducting ($\beta^{6.3}$-helical) dimers (D); $\beta^{6.3}$-helical monomers (M); and non-$\beta^{6.3}$-helical monomers (M′).

$$2M' \leftrightarrow 2M \leftrightarrow D$$

According to this scheme, the decreased channel appearance rate could result from a decrease in the monomer → dimer association rate constant, from a shift in M′/M equilibrium toward the M′ form, or from a combination of these effects. It is in this respect relevant that gramicidin monomers in organic solvents are random coils (Roux et al., 1990), since an unfolded structure could be stabilized by the insertion of the acyl chain into the bilayer.

Identity of the Fatty Acids. Among the fatty acids in gramicidin K, the branched and straight C_{15} fatty acids are uncommon in mammals, but fairly common in bacteria. For *Bacillus subtilis*, *Bacillus cereus*, and *Bacillus megaterium*, in fact, 12-methyltetradecanoic acid is the most abundant fatty acid and constitutes >40% of total fatty acids (Asselineau, 1966). Both the branched methyl resonance at 19.0 ppm in the ^{13}C-NMR spectrum (Figure 11 and Table II) and the mass spectrum (Figure 10) confirm 12-methyltetradecanoic acid as one of the major fatty acid components of acylated gramicidins from *B. brevis*.

The relative proportions of branched and unbranched fatty acids present in the original acylgramicidin mixture is uncertain. Although the relative intensity of the 19.0 ppm resonance with respect to the four Val-γ_1 resonances and the 11.1 ppm terminal methyl resonance suggests that a major fraction of the acyl chains are branched, the NMR peak intensities were not quantitative under the given experimental conditions. The chromatogram of Figure 9 suggests that 12-methyltetradecanoic acid and hexadecanoic acid each represent 30–35% of the acyl chains and that pentadecanoic acid and octadecanoic acid each represent 15–20%. In any case, the branched 12-methyltetradecanoic acid is a major component of acyl-gA and acyl-gC, consistent with its relative abundance in *Bacilli* in general.

Possible Implication for the Biological Function of Gramicidins. In addition to being potent membrane-active substances that increase the permeability of lipid bilayers and biological membranes to the alkali metal cations and H^+, the linear gramicidins are also inhibitors of RNA polymerase (Sarkar et al., 1979). Their function in the producing organism (*B. brevis*) is presumably related to the latter action. But this raises the question of why producers do not commit metabolic "suicide", through the production of gramicidin that would induce an uncoupling of their normal energy metabolism, in addition to whatever other changes in cell physiology the gramicidin induces. It is in this respect interesting to speculate that the acylated gramicidins may be the actual biosynthetic end product and that the standard gramicidins result from the hydrolysis of the ester at the rather alkaline pH in the broth (Hotchkiss, 1941). If that were the case, the lower channel-forming potency of the acylated gramicidins might also reflect a lesser ability of these compounds to increase the cation permeability of biological membranes, which would reduce the risk of metabolic uncoupling.

ACKNOWLEDGMENT

We thank Bas Vogt and Douglas Sawyer for stimulating discussions.

REFERENCES

Andersen, O. S. (1983a) *Biophys. J. 41*, 119–133.
Andersen, O. S. (1983b) *Biophys. J. 41*, 147–165.
Arseniev, A. S.; Barsukov, I. L., Bystrov, V. F.; Lomize, A. L., & Ovchinnikov, Y. A. (1985) *FEBS Lett. 186*, 168–174.
Arseniev, A. S., Lomize, A. L., Barsukov, I. L., & Bystrov, V. F. (1986) *Biol. Membr. 3*, 1077–1104.
Asselineau, J. (1966) *The Bacterial Lipids*, pp 235–237, Hermann, Paris.
Becker, M. D., Koeppe, R. E., II, & Andersen, O. S. (1992) *Biophys. J. 62*, 25–27.
Benayad, A., Benamar, D., Van Mau, N., Page, G., & Heitz, F. (1991) *Eur. Biophys. J. 20*, 209–213.
Benz, R., & Janko, K. (1976) *Biochim. Biophys. Acta 455*, 721–738.
Busath, D. D., Andersen, O. S., & Koeppe, R. E., II (1987) *Biophys. J. 51*, 79–88.
Cast, K. G., McPherson, J. K., Pollard, A. J., Krenzer, E. G., Jr., & Waller, G. R. (1990) *J. Chem. Ecol. 16*, 2277–2289.
Cifu, A., Koeppe, R. E., II, & Andersen, O. S. (1992) *Biophys. J. 61*, 189–203.
Cox, D. R., & Lewis, P. A. W. (1965) *The Statistical Analysis of Series of Events*, pp 1–16, Methuen, London.
Durkin, J. T., Koeppe, R. E., II, & Andersen, O. S. (1990) *J. Mol. Biol. 211*, 221–234.
Eight Peak Index of Mass Spectra (1983) Mass Spectrometry Data Centre, University of Nottingham, Royal Society of Chemistry, United Kingdom.
Etchebest, C., & Pullman, A. (1984) *FEBS Lett. 170*, 191–195.
Etchebest, C., & Pullman, A. (1986) *FEBS Lett. 204*, 261–265.
Etchebest, C., Ranganathan, S., & Pullman, A. (1984) *FEBS Lett. 173*, 301–356.
Hawkes, G. E., Lian, L. Y., Randall, E. W., Sales, K. D., & Curzon, E. H. (1987) *Eur. J. Biochem. 166*, 437–445.
Helfrich, P., & Jakobsson, E. (1990) *Biophys. J. 57*, 1075–1084.
Hotchkiss, R. D. (1941) *J. Biol. Chem. 141*, 171.
Huang, H. W. (1986) *Biophys. J. 50*, 1061–1070.
Koeppe, R. E., II, Paczkowski, J. A., & Whaley, W. L. (1985) *Biochemistry 24*, 2822–2826.
Koeppe, R. E., II, Corder, R. A., Andersen, O. S., Narcessian, E. J., Peart, L. M., & Waller, G. R. (1988) *Biophys. J. 53*, 328a.
Koeppe, R. E., II, Mazet, J.-L., & Andersen, O. S. (1990) *Biochemistry 29*, 512–520.
Koeppe, R. E., II, Providence, L. L., Greathouse, D. V., Heitz, F., Trudelle, Y., Purdie, N., & Andersen, O. S. (1992) *Proteins 12*, 49–62.
McGown, S. R., & Waller, G. R. (1986) *34th Annual Conference on Mass Spectrometry and Applied Topics*, pp 306–307, Cincinnati, OH.
McLafferty, F. W. (1959) *Anal. Chem. 31*, 82–87.
Nicholson, L. K., LoGrasso, P. V., & Cross, T. A. (1989) *J. Am. Chem. Soc. 11*, 400–401.
O'Connell, A. M., Koeppe, R. E., II, & Andersen, O. S. (1990) *Science 250*, 1256–1259.

Pullman, A. Jortner, J., & Pullman, B., Ed. (1988) *Transport through Membranes*: *Carriers, Channels and Pumps*, Kluwer Academic, Dordrecht, The Netherlands.

Roux, B., Brueschweiler, R., & Ernst, R. R. (1990) *Eur. J. Biochem. 194*, 57–60.

Russell, E. W. B., Weiss, L. B., Navetta, F. I., Koeppe, R. E., II, & Andersen, O. S. (1986) *Biophys. J. 49*, 673–686.

Sarges, R., & Witkop, B. (1965) *J. Am. Chem. Soc. 87*, 2011–2020.

Sarkar, N., Langley, D., & Paulus, H. (1979) *Biochemistry 18*, 4536–4541.

Sawyer, D. B., & Andersen, O. S. (1989) *Biochim. Biophys. Acta 987*, 129–132.

Sawyer, D. B., Koeppe, R. E., II, & Andersen, O. S. (1989) *Biochemistry 28*, 6571–6583.

Sawyer, D. B., Williams, L. P., Whaley, W. L., Koeppe, R. E., II, & Andersen, O. S. (1990) *Biophys. J. 58*, 1207–1212.

Segrest, J. P., & Feldmann, R. J. (1974) *J. Mol. Biol. 87*, 853–858.

Trudelle, Y., Daumas, P., Heitz, F., Etchebest, C., & Pullman, A. (1987) *FEBS Lett. 216*, 11–16.

Urry, D. W. (1971) *Proc. Natl. Acad. Sci. U.S.A. 68*, 672–676.

Vogt, T. C. B., Killian, J. A., de Kruijff, B., & Anderson, S. O. (1992) *Biochemistry* (following paper in this issue).

Williams, D. H., Budzikiewicz, H., & Djerassi, C. (1964) *J. Am. Chem. Soc. 86*, 284–287.

Williams, L. M. P., Narcessian, E. J., Andersen, O. S., & Koeppe, R. E., II (1988) *Biophys. J. 53*, 329a.